Radiative Heat Transfer in Absorbing, Emitting, and Anisotropically Scattering Boundary-Layer Flows

Adnan Yücel*
University of Mississippi, University, Mississippi
and
Yildiz Bayazitoğlu†
Rice University, Houston, Texas

The effect of scattering on heat transfer in boundary-layer flows over a flat plate, over a 90-deg wedge, and in stagnation flow is investigated. To this end, a linear anisotropic scattering model is employed. The *P*-3 and *P*-1 approximation methods are used to analyze the radiation part of the problem. The complete nonsimilar boundary-layer equations are solved by an implicit collocation procedure. Comparisons with the existing exact results for the case of isotropic scattering show that, overall, the *P*-3 approximation is more accurate than the *P*-1 approximation in predicting the total heat flux at the wall. Scattering generally leads to a reduction in the total heat flux. The degree of anisotropy can have a significant effect on the heat transfer in the boundary layer. The total heat flux for a forward-scattering fluid can be greater than that for a nonscattering fluid, depending on the value of the scattering albedo and the forward-backward scattering parameter.

Nomenclature

a = forward-backward scattering parameter
B = dimensionless blackbody emissive power, θ^4
e_b = blackbody emissive power, $\bar{\sigma}T^4$
f = dimensionless stream function
i = intensity of radiation
i_k, I_k = kth moment of intensity given by Eq. (6), $I_k = i_k/4\bar{\sigma}T_\infty^4$
k = thermal conductivity
N = conduction-radiation parameter, $k(\kappa+\sigma)/4\bar{\sigma}T_\infty^3$
m = constant, $\alpha/(2\pi+\alpha)$
Nu_x = local Nusselt number
p = phase function
P_n = Legendre polynomial of the first kind of degree n
Pr = Prandtl number
q_r, Q_r = radiative heat flux, $Q_r = q_r/4\bar{\sigma}T_\infty^4$
q_w, Q_w = total heat flux at the wall, $Q_w = q_w/4\bar{\sigma}T_\infty^4$
Re_x = Reynolds number, $U_\infty(x)x/\nu$
T = temperature
T_w = wall temperature
T_∞ = external flow temperature
$U_\infty(x)$ = external flow velocity, $\sim x^m$
x,y = physical coordinates along and normal to the wall
α = wedge angle, rad
β = polar angle
ζ = nonsimilarity variable, $(\kappa+\sigma)x/Re_x^{1/2}$
η = similarity variable, $yRe_x^{1/2}/x$
θ = dimensionless temperature, T/T_∞
θ_w = dimensional wall temperature, T_w/T_∞
κ = absorption coefficient
λ = scattering albedo
μ = direction cosine, $\cos\beta$
σ = scattering coefficient
$\bar{\sigma}$ = Stefan-Boltzmann constant
τ = optical variable, $(\kappa+\sigma)y$
Ω = solid angle

Received July 21, 1983; revision submitted Oct. 10, 1983.

*Visiting Assistant Professor.
†Associate Professor. Member AIAA.

Introduction

At high temperatures, thermal radiation can significantly affect the heat transfer and the temperature distribution in the boundary-layer flow of a participating fluid. A complete analysis of the interaction of radiation with the boundary-layer flow involves the solution of a nonlinear integrodifferential equation.[1] Such exact treatment of the problem requires considerable effort and large amounts of computing time that can be prohibitive.[2] In the past, various simplifications have been introduced to overcome the mathematical complexity of the problem. The optically thin limit and the optically thick limit approximations have been used by several investigators.[3-6] These approximations are accurate only within particular optical thickness limits and, therefore, are restricted in applicability. The exponential kernel approximation and the differential approximation have also been utilized.[7,8] The introduction of a realistic phase function to describe the angular distribution of scattered energy complicates the analysis further. Only a few of these studies have studied the relatively simple case of isotropic scattering, and none have considered anisotropic scattering effects.

The objective of this investigation is to demonstrate the influence of anisotropic scattering on the boundary-layer flow of a participating fluid over a wedge. To this effect, the *P*-3 approximation is used to solve the radiation part of the problem, and the linear anisotropic scattering model is em-

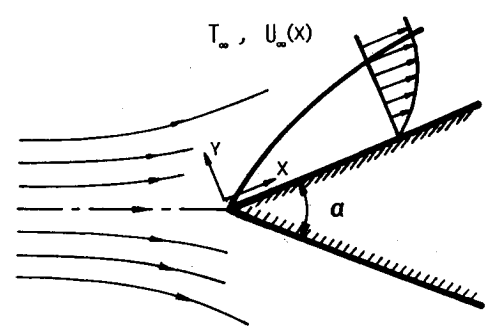

Fig. 1 Schematic illustration of the physical system.

ployed. The *P-N* approximation method, also known as the spherical harmonics method, is capable of generating higher-order approximate solutions to the equation of radiative transfer. The *P*-3 approximation is superior to the *P*-1 (differential) approximation and it yields accurate results over a wide range of optical thickness in pure radiation and combined conduction and radiation problems in plane parallel geometry.[9,10] The linear anisotropic model was found to work well in treating Mie anisotropic scattering in planar media.[11] A slightly modified form of the differential approximation was also considered in Ref. 11. The linear model was introduced into the *P*-3 approximation to study radiative transfer in anisotropically scattering media between concentric cylinders and spheres.[12]

Analysis

The physical model under consideration consists of an incompressible, constant property, gray fluid flowing over a black surface wedge held at uniform temperature T_w, as shown in Fig. 1. The external flow is at constant temperature T_∞ and its velocity $U_\infty(x)$ is given by

$$U_\infty(x) = Cx^m, \qquad m = \alpha/(2\pi - \alpha)$$

where α is the wedge angle in radians and C is a constant. Specifically, the cases $m = 0, \frac{1}{3}$, and 1 correspond to flow over a flat plate, over a 90-deg wedge, and stagnation flow, respectively. The fluid absorbs, emits, and scatters radiation and has a refractive index of unity. Steady state is assumed and viscous energy dissipation is neglected. Under these considerations, the momentum and energy equations in the boundary layer are[1]

$$f''' + \frac{1+m}{2} ff'' + m[1 - (f')^2] = 0 \tag{1a}$$

$$\theta'' + \frac{1+m}{2} Prf\theta' - \frac{1-m}{2} Prf'\zeta \frac{\partial\theta}{\partial\zeta} - \frac{\zeta}{N} Q_r' = 0 \tag{1b}$$

subject to the boundary conditions

$$\eta = 0 \qquad f = f' = 0 \qquad \theta = \theta_w \tag{2a}$$

$$\eta \to \infty \qquad f' = 1 \qquad \theta = 1 \tag{2b}$$

where the prime denotes differentiation with respect to the similarity variable $\eta = Re_x^{1/2} y/x$, and $f(\eta)$ and $\theta(\eta, \zeta)$ represent the dimensionless stream and temperature functions. Unlike the velocity boundary layer, the thermal boundary layer is not similar, with the temperature function θ depending on two independent variables η and ζ. The latter variable ζ, defined as $\zeta = (\kappa + \sigma)x/Re_x^{1/2}$, is a measure of the optical thickness of the boundary layer, which is said to be optically thin when $\zeta \ll 1$ and optically thick when $\zeta \gg 1$. The radiation part of the problem satisfies the equation of radiative transfer given in the form[1]

$$\mu \frac{\partial i}{\partial \tau} = -i + (1-\lambda)\frac{e_b}{\pi} + \frac{\lambda}{2}\int_{-1}^{1} ip(\mu, \mu')\, d\mu' \tag{3}$$

The phase function p in Eq. (3) can be expanded in a series of the form[13]

$$p(\mu, \mu') = \sum_{n=0}^{\infty} a_n P_n(\mu \cdot \mu'), \qquad a_0 = 1 \tag{4a}$$

In the following analysis, the phase function is replaced by a linear function on grounds of simplicity

$$p(\mu, \mu') = 1 + a\mu \cdot \mu' \tag{4b}$$

which can be refined as described in Ref. 11.

In the *P-N* approximation, the angular distribution of the intensity of radiation is represented by a series of associated Legendre polynomials of the first kind. The series is truncated after N terms and the coefficients are expressed in terms of the moments of intensity. The equations governing the moments of intensity are obtained by multiplying Eq. (3) by the appropriate powers of the direction cosine μ and subsequently integrating over a solid angle of 4π. The moment differential equations so obtained for the *P*-3 approximation are

$$\frac{\partial i_1}{\partial \tau} = (1-\lambda)(4e_b - i_0) \tag{5a}$$

$$\frac{\partial i_2}{\partial \tau} = -\left(1 - \frac{\lambda a}{3}\right) i_1 \tag{5b}$$

$$\frac{\partial i_3}{\partial \tau} = -i_2 + \frac{1}{3} i_0 + \frac{1-\lambda}{3}(4e_b - i_0) \tag{5c}$$

$$\frac{\partial i_4}{\partial \tau} = -i_3 + \frac{\lambda a}{5} i_1 \tag{5d}$$

where $\tau = (\kappa + \sigma)y$. The kth moment of intensity is defined as

$$i_k = \int_{4\pi} i\mu^k \, d\Omega, \qquad k = 0, 1, \ldots, N \tag{6}$$

Of particular interest is the first moment of intensity which is identical to the radiative flux in the y direction. Equations (5a) and (5b) represent the moment equations for the *P*-1 approximation. The closure condition to evaluate the $N+1$th moment of intensity is

$$i_4 = 6i_2/7 - 3i_0/35 \tag{7a}$$

for the *P*-3 approximation and

$$i_2 = i_0/3 \tag{7b}$$

for the *P*-1 approximation.

The boundary conditions for the *P*-3 approximation obtained by the Marshak approach are[9,10]

$$3i_0 \pm 16i_1 + 15i_2 - 32e_b = 0 \tag{8a}$$

$$-2i_0 + 30i_2 \pm 32i_3 - 32e_b = 0 \tag{8b}$$

where the plus sign corresponds to $y = 0$ and the minus sign corresponds to $y \to \infty$. The boundary conditions for the *P*-1 approximation can be obtained by introducing Eq. (7b) into Eq. (8a).

Substituting the respective closure conditions given by Eqs. (7) in the moment differential equations, and after some algebraic manipulation, one obtains the following dimensionless equations

$$I_0'' + \zeta^2\{(1-\lambda)(55/9 - \lambda a)B(\theta) - [35\lambda/9 + (10 - \lambda a)(1-\lambda)]I_0 + 35I_2/3\} = 0 \tag{9a}$$

$$I_2'' + \zeta^2(1 - \lambda a/3)(1-\lambda)[B(\theta) - I_0] = 0 \tag{9b}$$

for the *P*-3 approximation and

$$I_0'' + \zeta^2(3 - \lambda a)(1-\lambda)[B(\theta) - I_0] = 0 \tag{10}$$

for the *P*-1 approximation. The radiative flux term in the energy equation is given by

$$Q_r' \equiv I_1' = \zeta(1-\lambda)[B(\theta) - I_0] \tag{11}$$

The energy equation and Eqs. (9) or (10), together with the respective boundary conditions, constitute the system of differential equations to be solved simultaneously. After the temperature and radiative flux distributions are determined for a given set of values of the system parameters m, Pr, N, θ_w, λ, and a, the net heat flux at the wall can be evaluated by

$$q_w = \left[-k\frac{\partial T}{\partial y} + q_r\right]_{y=0} \tag{12}$$

In terms of the dimensionless quantities, Eq. (12) is expressed as

$$Q_w = \left[-\frac{N}{\zeta}\theta' + Q_r\right]_{\eta=0} \tag{13}$$

The total heat flux is related to the Nusselt number along the boundary by

$$-\frac{\zeta}{N}Q_w = (1-\theta_w)Nu_x Re_x^{-1/2} \tag{14}$$

Solution Method

The values of f and f' needed in the energy equation were obtained by solving the momentum equation for different values of m using the modified quasilinearization algorithm for nonlinear two-point boundary-value problems.[14] The maximum value of η was set as $\eta = 20$ and a uniform grid of 100 divisions was used throughout this study. The outer boundary conditions were satisfied well before $\eta = 20$. The partial derivative of the temperature, with respect to ζ in the energy equation, was replaced by a backward finite difference formula. The resulting system of nonlinear second-order ordinary differential equations for the temperature and the even moments of intensity were reduced to a nonlinear system of equations by a collocation procedure. Cubic Hermite polynomials were employed as interpolating functions to obtain accurate representations of the temperature gradient and the radiative flux at the surface. The system of equations was solved by the modified quasilinearization algorithm.[15] The algorithm was stopped when the value of the per-

Table 1 Comparative results for the temperature gradient, radiative flux, and the total heat flux on the wall in flow of an isotropically scattering fluid over a 90-deg wedge with $Pr = 1.0$, $N = 0.1$

λ	ζ	$\theta'\|_{\eta=0}$			$-Q_r\|_{\eta=0}$			$-(\zeta/N)Q_w$		
					$\theta_w = 0.1$					
		Exact[2]	*P*-3	*P*-1	Exact	*P*-3	*P*-1	Exact	*P*-3	*P*-1
0.0	0.005	0.396	0.396	0.396	0.140	0.247	0.250	0.403	0.409	0.409
	0.025	0.397	0.398	0.398	0.203	0.229	0.239	0.448	0.455	0.458
	0.050	0.401	0.403	0.403	0.193	0.205	0.216	0.498	0.505	0.512
	0.075	0.407	0.410	0.412	0.177	0.183	0.193	0.540	0.547	0.556
	0.100	0.414	0.418	0.421	0.160	0.163	0.172	0.574	0.581	0.593
	0.200	0.446	0.453	0.464	0.107	0.106	0.108	0.660	0.665	0.680
0.75	0.005	0.396	0.396	0.396	0.098	0.235	0.237	0.401	0.408	0.408
	0.025	0.396	0.396	0.396	0.121	0.197	0.202	0.426	0.446	0.447
	0.050	0.396	0.397	0.397	0.146	0.172	0.177	0.469	0.483	0.486
	0.075	0.398	0.398	0.398	0.143	0.157	0.162	0.504	0.515	0.519
	0.100	0.398	0.399	0.399	0.137	0.145	0.150	0.535	0.544	0.550
	0.200	0.403	0.406	0.408	0.110	0.112	0.115	0.623	0.631	0.639
	0.250	0.408	0.411	0.414	0.098	0.100	0.102	0.653	0.660	0.669
					$\theta_w = 0.7$					
		Exact	*P*-3	*P*-1	Exact	*P*-3	*P*-1	Exact	*P*-3	*P*-1
0.0	0.005	0.132	0.132	0.132	0.126	0.189	0.191	0.138	0.142	0.142
	0.025	0.132	0.132	0.133	0.162	0.179	0.187	0.173	0.177	0.179
	0.050	0.133	0.134	0.134	0.157	0.165	0.174	0.212	0.217	0.221
	0.075	0.135	0.136	0.137	0.147	0.152	0.160	0.245	0.250	0.257
	0.100	0.137	0.139	0.140	0.136	0.139	0.156	0.273	0.276	0.287
	0.200	0.147	0.149	0.155	0.100	0.100	0.103	0.346	0.349	0.361
0.4	0.005	0.132	0.132	0.132	0.112	0.184	0.186	0.138	0.141	0.141
	0.025	0.132	0.132	0.132	0.143	0.167	0.175	0.168	0.174	0.175
	0.050	0.132	0.132	0.133	0.144	0.154	0.161	0.204	0.209	0.213
	0.075	0.132	0.133	0.133	0.137	0.142	0.150	0.235	0.240	0.246
	0.100	0.133	0.134	0.135	0.130	0.133	0.139	0.262	0.267	0.274
	0.200	0.137	0.138	0.141	0.099	0.101	0.104	0.336	0.340	0.350
0.75	0.005	0.132	0.132	0.132	0.089	0.178	0.181	0.136	0.141	0.141
	0.025	0.132	0.132	0.132	0.098	0.151	0.155	0.156	0.170	0.171
	0.050	0.131	0.132	0.132	0.116	0.134	0.138	0.190	0.199	0.201
	0.075	0.131	0.131	0.131	0.114	0.124	0.128	0.217	0.224	0.226
	0.100	0.130	0.131	0.131	0.111	0.117	0.121	0.241	0.248	0.252
	0.200	0.128	0.129	0.130	0.094	0.095	0.098	0.315	0.319	0.326
0.95	0.005	0.132	0.132	0.132	0.051	0.176	0.176	0.134	0.141	0.141
	0.025	0.132	0.132	0.132	0.051	0.139	0.142	0.145	0.167	0.167
	0.050	0.132	0.132	0.132	0.057	0.113	0.116	0.160	0.188	0.190
	0.075	0.131	0.132	0.132	0.067	0.098	0.100	0.181	0.205	0.207
	0.100	0.131	0.131	0.131	0.067	0.088	0.090	0.198	0.217	0.222
	0.200	0.128	0.129	0.129	0.067	0.070	0.071	0.257	0.267	0.271

formance index which represents the total error in the system was less than 10^{-16}. Details of the procedure can be found in Ref. 16. Initially the solutions for the nonradiating thermal boundary layer ($\zeta=0$) were obtained. The system of equations was then solved for increasing values of ζ. For each new ζ value, the converged solutions at the preceding value of ζ were used as initial guesses for the temperature and the moments of intensity. No more than three iterations were required to achieve convergence.

In stagnation flow, i.e., when $m=1$, the partial derivative of θ with respect to ζ vanishes and the energy equation reduces to a local similar form in terms of ζ. The system of equations can be solved for different values of ζ independent of the "upstream" solutions in this case.

Results and Discussion

In order to keep the number of independent parameters to a minimum, the present consideration is limited only to those cases with $Pr=1$. The results presented are obtained by the P-3 approximation method unless otherwise noted. The scattering effects are represented by the scattering albedo λ ($0\le\lambda\le1$) and the forward-backward scattering parameter a. The limiting values of the scattering albedo signify a purely absorbing fluid ($\lambda=0$) and a purely scattering fluid ($\lambda=1$). The forward-backward scattering parameter is a measure of the degree of anisotropy. In this study its values are restricted to the range $-1\le a\le1$; results are presented for the two limiting values $a=-1$ and 1 which represent cases of strong backward and strong forward scattering, respectively. The results for intermediate values of a lie between these two cases. Obviously, $a=0$ implies isotropic scattering for $\lambda\neq0$.

Table 1 gives the temperature gradient, the radiative flux, and the total heat flux at the wall for an isotropically scattering fluid, obtained from the exact calculations using the normal-mode expansion technique[2] and the P-3 and P-1 approximation methods. The results presented are for the case of boundary-layer flow over a 90-deg wedge ($m=\frac{1}{3}$) with $\theta_w=0.1$ and 0.7 and various values of the scattering albedo. The effect of the scattering albedo is to decrease the total heat flux at the wall. This is due to the fact that the temperatures tend to pure convection temperatures with increasing values of λ as this implies less interaction (for $\lambda=1$: decoupling) of radiation with the thermal boundary layer. The P-3 and P-1 approximation results generally follow the same trends as the exact results. Both approximations tend to overpredict the radiative and conductive heat fluxes and, consequently, the total flux at the wall. For optically thin boundary layers, i.e., $\zeta\ll1$, the approximate results for the radiative flux do not agree with the exact results, while they are accurate for relatively large values of ζ. It should be noted that both approximations predict the optically thick limit correctly. Overall, the total heat flux results are in good agreement and improve with increasing ζ. In all cases considered, the P-3 approximation results are found to be more accurate than the P-1 approximation results, especially for intermediate ζ values.

The scattering effects on heat transfer in the boundary-layer flow over a flat plate ($m=0$), over a 90-deg wedge ($m=\frac{1}{3}$), and in stagnation flow ($m=1$) are illustrated in Fig. 2. The reduction in the total heat flux due to isotropic scattering at first increases with ζ, but vanishes for optically thick boundary layers as would be expected. The forward-backward scattering parameter has a significant effect on the heat transfer. In the boundary-layer flow over a flat plate ($m=0$), for example, the total heat flux for a strong backward-scattering fluid ($a=-1$) with $\lambda=0.75$ is about 7% less than that for a strong forward-scattering fluid for $\zeta=0.1$, and 17% less for $\zeta=0.5$. The respective precentages are 5 and 12% in stagnation flow ($m=1$). Another interesting observation is that, unlike the isotropic scattering case, the total heat flux for a strong forward-scattering fluid can become greater than that for a nonscattering fluid, depending on the values of λ and a. Similar tendencies were discussed in Ref. 17 for the combined conduction and radiation problem. Viewing the parameter $\zeta=(\kappa+\sigma)x/Re_x^{1/2}$ as the dimensionless distance from the leading edge, it is observed that this phenomenon takes place in stagnation flow at a location further downstream than that in flow over a flat plate. The location in the case of flow over a 90-deg wedge lies in between.

With increasing ζ, the total heat flux tends to the optically thick limit. Again it is seen that this limit is attained sooner in flow over a flat plate than in stagnation flow. Furthermore, backward scattering is found to aid this process, while forward scattering has a retarding effect.

Figure 3 shows the variation of the wall heat flux with the conduction-radiation parameter N, which characterizes the relative importance of radiation in regard to conduction. The results are presented for flow over a flat plate and stagnation flow with $\theta_w=0.1$ and $\zeta=0.3$. It is observed that the local Nusselt number increases as N decreases (i.e., radiation increases). Anisotropic scattering effects on the heat flux are amplified at small values of N. They are found to be negligible for $N\ge1$. For this reason, the range of N in the figure is

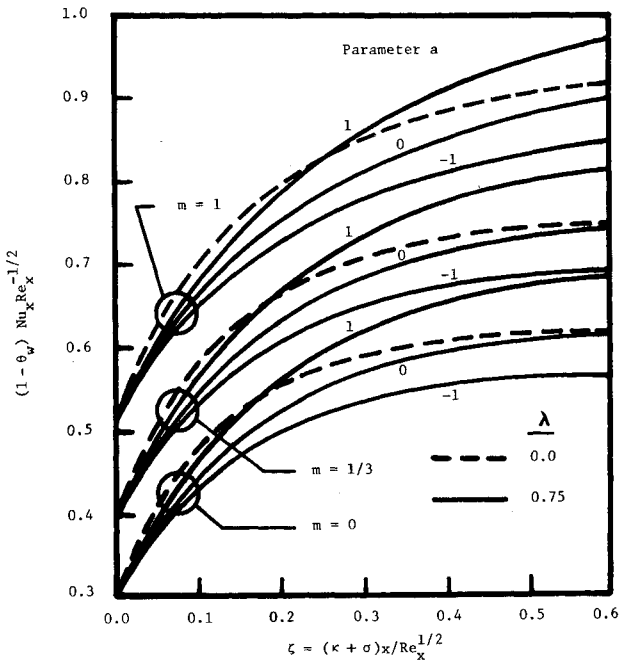

Fig. 2 The effect of scattering on the total heat flux at the wall vs ζ for flow over a flat plate ($m=0$), over a 90-deg wedge ($m=\frac{1}{3}$), and stagnation flow ($m=1$) with $Pr=1$, $N=0.1$, and $\theta_w=0.1$.

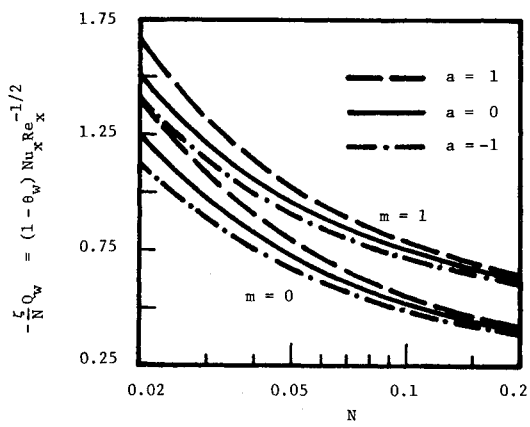

Fig. 3 Variation of the total wall heat flux with N at $\zeta=0.3$ for flow over a flat plate ($m=0$) and stagnation flow ($m=\frac{1}{3}$) with $Pr=1$, $\theta_w=0.1$, and $\lambda=0.75$.

truncated at $N=0.2$ although results were obtained by varying N from 0.01 to 10.

Finally, it was found that the temperature profiles in the boundary layer were not altered significantly by anisotropic scattering within the range of parameters involved. The temperatures for various values of the forward-backward scattering parameter deviate only slightly from those for the case of isotropic scattering ($a=0$) and therefore do not warrant publication since the latter are discussed thoroughly in the literature.

Conclusions

The P-3 and P-1 approximation methods are used to study the interaction of radiation with three different boundary-layer flows of an anisotropically scattering fluid. These approximations offer mathematical simplicity and require considerably less computation in comparison to an exact treatment of the problem. The P-3 approximation gives quite accurate results for the net wall heat flux in the isotropic scattering case. Overall, it is superior to the P-1 approximation. Both approximations are accurate in the optically thick range in which case the use of the P-1 approximation should be sufficient. Because of the large number of parameters involved, the conduction-radiation parameter is set at $N=0.1$ (relatively strong radiation effects) in this investigation. It is known from studies on the interaction of radiation with conduction in one-dimensional planar media that the greatest discrepancies between the results of the two approximations occur when radiation is the dominant mode ($N \ll 1$). The P-3 approximation should be utilized in such situations.

A linear phase function is employed to describe anisotropic scattering in the medium. However, both approximations (in general, the P-N approximation) are capable of accommodating more realistic phase functions for particular applications. Scattering generally decreases the total heat flux at the wall. The forward-backward scattering parameter can significantly affect the heat transfer in the boundary layer. Depending on the scattering albedo and the degree of anisotropy, the total heat flux can be greater than that for a nonscattering medium.

References

[1] Özisik, M. N., *"Radiative Transfer and Interactions with Conduction and Convection,"* Wiley-Interscience, New York, 1973.

[2] Boles, M. A., "Interactions of Radiation with Conductive and Convective Heat Transfer in Ablation and Boundary Layer Flow," Ph.D. Dissertation, Mechanical and Aerospace Engineering Department, North Carolina State University, Raleigh, N.C., 1972.

[3] Cess, R. D., "The Interaction of Thermal Radiation with Conduction and Convection Heat Transfer," *Advances in Heat Transfer,* edited by T. F. Irvine and J. P. Hartnett, Vol. 1, Academic Press, New York, 1964, pp. 1-50.

[4] Cess, R. D., "Radiation Effects Upon Boundary Layer Flow of an Absorbing Gas," *Journal of Heat Transfer*, Vol. 86C, Nov. 1964, pp. 469-475.

[5] Viskanta, R. and Grosh, R. J., "Boundary Layer in Thermal Radiation Absorbing and Emitting Media," *International Journal of Heat and Mass Transfer,* Vol. 5, Sept. 1962, pp. 795-806.

[6] Novotny, J. L. and Yang, K-T., "The Interaction of Thermal Radiation in Optically Thick Boundary Layers," ASME Paper 67-HT-9, 1967.

[7] Pai, S. I. and Tsao, C. K., "A Uniform Flow of a Radiating Gas Over a Flat Plate," *Proceedings of the Third International Heat Transfer Conference*, Vol. 5, Chicago, Ill., 1966, pp. 129-137.

[8] Bergquam, J. B., "Heat Transfer by Convection and Radiation in Laminar Boundary Layer Flow," *Proceedings of the Fifth International Heat Transfer Conference*, Vol. 5, Tokyo, 1974, pp. 83-87.

[9] Bayazitoğlu, Y. and Higenyi, J., "Higher Order Differential Equations of Radiative Transfer: P-3 Approximation," *AIAA Journal,* Vol. 17, April 1979, pp. 424-431.

[10] Ratzel, A. C. and Howell, J. R., "Heat Transfer by Conduction and Radiation in a One-Dimensional Planar Medium Using the Differential Approximation," *Journal of Heat Transfer,* Vol. 104, May 1982, pp. 388-391.

[11] Modest, M. F. and Azad, F. H., "The Influence and Treatment of Mie-Anisotropic Scattering in Radiative Heat Transfer," *Journal of Heat Transfer,* Vol. 102, Feb. 1980, pp. 92-98.

[12] Yücel, A. and Bayazitoğlu, Y., "Radiative Transfer in Anisotropically Scattering Nonplanar Media," *AIAA Journal*, Vol. 19, April 1981, pp. 540-542.

[13] Chu, C. M. and Churchill, S. W., "Representation of an Angular Distribution of Radiation Scattered by a Spherical Particle," *Journal of the Optical Society of America,* Vol. 45, Nov. 1955, pp. 958-962.

[14] Miele, A. and Iyer, R. R., "General Technique for Solving Non-Linear Two Point Boundary-Value Problems Via the Method of Particular Solutions," *Journal of Optimization Theory and Applications,* Vol. 5, May 1970, pp. 382-399.

[15] Miele, A., Naqvi, S. and Levy, A. V., "Modified Quasilinearization Method for Solving Nonlinear Equations," Aero-Astronautics Report 78, Rice University, Houston, Tex., 1970.

[16] Yücel, A., "P-N Approximation for Radiative Transfer in a Nongray Planar Medium," Ph.D. Dissertation, Rice University, Houston, Tex., 1982.

[17] Yuen, W. W. and Wong, L. W., "Heat Transfer by Conduction and Radiation in a One-Dimensional Absorbing, Emitting and Anisotropically-Scattering Medium," *Journal of Heat Transfer,* Vol. 102, May 1980, pp. 303-307.